International Journal of Humanoid Robotics
Vol. 8, No. 1 (2011) 169–183

DOI: 10.1142/S0219843611002381

World Scientific
www.worldscientific.com

STEREOVISION-BASED FUZZY OBSTACLE AVOIDANCE METHOD

LAZAROS NALPANTIDIS* and ANTONIOS GASTERATOS†

Robotics and Automation Laboratory,
Production and Management Engineering Department,
Democritus University of Thrace,
University Campus, Kimmeria, GR-671 00 Xanthi, Greece
**lanalpa@pme.duth.gr*
†*agaster@pme.duth.gr*

Received 5 July 2010
Accepted 7 August 2010

This work presents a stereovision-based obstacle avoidance method for autonomous mobile robots. The decision about the direction on each movement step is based on a fuzzy inference system. The proposed method provides an efficient solution that uses a minimum of sensors and avoids computationally complex processes. The only sensor required is a stereo camera. First, a custom stereo algorithm provides reliable depth maps of the environment in frame rates suitable for a robot to move autonomously. Then, a fuzzy decision making algorithm analyzes the depth maps and deduces the most appropriate direction for the robot to avoid any existing obstacles. The proposed methodology has been tested on a variety of self-captured outdoor images and the results are presented and discussed.

Keywords: Fuzzy obstacle avoidance; stereo vision; autonomous robot navigation.

1. Introduction

Robotics often replicate human modalities in order to achieve autonomous behaviors.[1] Above all, vision is the most important sense to humans; moreover, we have structured our environments based on this fact. It comes, therefore, naturally that robots can be greatly benefited by employing vision methods.[2] In this work, a vision-based fuzzy obstacle avoidance algorithm is presented that is suitable for autonomous mobile robots. The development of an efficient and solely vision-based method for mobile robot navigation is still an active research topic. Towards this direction, the first step is to ensure that any collisions will be avoided through vision. However, systems placed on robots have to conform to the restrictions imposed by them. Autonomous robot navigation requires almost real-time frame rates from the responsible algorithms. Furthermore, computing resources are strictly limited onboard a robot. Thus, avoiding the use of popular but calculation intensive obstacle

detection techniques such as the v-disparity image calculation, which afterwards require Hough-transformations, would be highly appreciated. Instead, simple and efficient solutions are demanded.

In order to achieve reliable obstacle avoiding behavior, many popular methods involve the use of artificial stereo vision systems. As affirmed by its biomimetic origin,[3,4] stereoscopic vision can be effectively used in order to derive the depth map of a scene. The three-dimensional position of the depicted objects can be obtained by two simultaneously captured and slightly misplaced views of a scene. Mobile robots can take advantage of stereo vision systems as a reliable method to extract information about their environment.[5] Despite the fact that stereo vision provides an enormous amount of information, most of the mobile robot navigation systems use complementary sensors in order to navigate safely.[6] The use of lasers, projectors, and various other range finders is a commonplace. The goal of this work is to develop a real-time obstacle avoidance algorithm based only on a stereo camera, for autonomous mobile robots. The core of the presented approach can be divided into two separate and independent algorithms:

- *The stereo vision algorithm*: It retrieves information about the environment from a stereo camera and produces a dense depth image, i.e. disparity map, of the scene.
- *The fuzzy decision making algorithm*: It analyzes the data of the previous algorithm and decides the best direction for the robot to move, so as to avoid any existing obstacles, based on a simple fuzzy inference system (FIS).

This section serves as an introduction referencing previously published related works and giving a brief overview of the proposed new method. The rest of the article is organized as follows: Sec. 2 describes the custom-developed stereo correspondence algorithm, Sec. 3 presents the FIS used for the obstacle analysis and the direction decision, Sec. 4 presents experimental results obtained using the proposed method, and finally Sec. 5 concludes this work highlighting the most interesting points.

1.1. *Related works*

Autonomous robots' behavior greatly depends on the accuracy of their decision-making algorithms. In the case of stereo vision-based navigation, the accuracy and the refresh rate of the computed disparity maps are the cornerstone of its success.[7] Dense local stereo correspondence methods calculate depth for almost every pixel of the scenery, talking into consideration only a small neighborhood of pixels each time.[8] On the other hand, global methods are significantly more accurate but at the same time more computationally demanding, as they account for the whole image.[9] However, since the most urgent constraint in autonomous robotics is the real-time operation, such applications usually utilize local algorithms. Muhlmann *et al.*[10] describe a local method that uses the sum of absolute differences (SAD) correlation measure for RGB color images. Applying a left-to-right consistency check,

the uniqueness constraint and a median filter, it can achieve 20 fps, for 160×120 pixel images. Another fast local AD-based algorithm is presented by Di Stefano and his colleagues.[11] It is based on the uniqueness constraint and rejects previous matches as soon as better ones are detected. It achieves 39.59 fps for 320×240 pixel images with 16 disparity levels and the root mean square error for the standard Tsukuba pair is 5.77. The algorithm reported by Yoon achieves almost real-time performance.[12] It is once more based on SAD but the correlation window size is adaptively chosen for each region of the picture. Apart from that, a left-to-right consistency check and a median filter are utilized. The algorithm is able to compute 7 fps for 320×240 pixel images with 32 disparity levels. Another possibility in order to obtain accurate results in real-time is to utilize programmable graphic processing units (GPU). A hierarchical disparity estimation algorithm is presented.[13] This method can process either rectified or noncalibrated image pairs using a local SAD-based bidirectional process. This algorithm is implemented on an ATI Radeon 9,700 Pro GPU and can achieve up to 50 fps for 256×256 pixel input images. On the other hand, an interesting but very computationally demanding local method is presented by Yoon.[14] It uses varying weights for the pixels in a given support window, based on their color similarity and geometric proximity. However, the execution speed of the algorithm is far from being real-time. The running time for the Tsukuba image pair with a 35×35 pixels support window is about one minute. The error ratio is only 1.29%, 0.97%, 0.99%, and 1.13% for the Tsukuba, Sawtooth, Venus, and Map image sets accordingly. A detailed taxonomy and presentation of dense stereo correspondence algorithms can be found by Scharstein and Szeliski.[8] Additionally, the recent advances in the field as well as the aspect of hardware implementable stereo algorithms are covered.[15]

As far as obstacle avoidance techniques are concerned, a wide range of sensors and various methods have been proposed in the relevant literature. Some interesting details about the developed sensor systems and proposed detection and avoidance algorithms can be found.[16,17] Movarec has proposed the certainty grid method[18] and Borenstein has proposed the virtual force field method[19] for robot obstacle avoidance. Then, the elastic strips method was proposed[20,21] treating the trajectory of the robot as an elastic material to avoid obstacles. Moreover, Choi has presented a modified elastic strip method for mobile robots operating in uncertain environments.[22] Reviews of popular obstacle avoidance algorithms covering them in more detail can be found.[23,24] Finally, the concept of using fuzzy logic for obstacle avoidance purposes was covered by Reignier, but only up to a theoretical level.[25]

The obstacle avoidance systems found in literature involve the use of one or a combination of ultrasonic, laser, infrared (IR), or vision senors. The use of ultrasonic, laser, and IR sensors is well studied and the depth measurements are quite accurate and easily available. However, such sensors suffer either from achieving only low refresh rates,[26] or being extremely expensive. On the other hand, vision sensors, either monocular, stereo, or multicamera ones, can combine high frame rates and appealing prices.

Stereo vision is often used in vision-based methods, instead of monocular sensors, due to the simpler calculations involved in the depth estimation. Regarding stereo vision systems, one of the most popular methods for obstacle avoidance is the initial estimation of the so-called v-disparity image. This method requires plenty of complex calculations and is applied in order to confront the noise in low quality disparity images.[27–29] However, if detailed and noise-free disparity maps were available, less complicated methods could have been used instead. Considering the above as a background, the contribution of this work is the development and experimental testing of a lightweight fuzzy algorithm for obstacle avoidance with the sole use of a stereoscopic camera. The use of only one sensor and especially of a stereoscopic camera diminish the complexity of our system and can also be easily integrated and interact with other stereo vision tasks such as object recognition and tracking.

1.2. *Proposed method overview*

The proposed method processes each pair of stereoscopic images and indicates an obstacle-avoiding direction of movement for a robot, such as the one shown in Fig. 1(a) or any humanoid robot as long as it is equipped with a stereo camera. First, the stereo image pair is given as input to a *stereo vision* algorithm and a depth map of the scene is obtained. This depth map is thereafter used as input of the *fuzzy obstacle analysis and direction decision* module. This fuzzy module indicates the proper direction of movement. The direction of movement ranges from −30° to +30°, considering 0° as the direction the robot is heading to. This angle range is dictated by the used stereo camera, i.e. a Bumblebee2 stereo camera manufactured by Point Grey Research, having a 60° horizontal field of view (HFoV). Furthermore, in cases when the scene is full of obstacles or the depth map is too noisy to conclude safely a "move backwards" signal is foreseen. Figure 1(b) presents the mobile robot, shown as the "R" in the center, and the possible positions after the application of the proposed algorithm, shown by the bold regions of the outer circle.

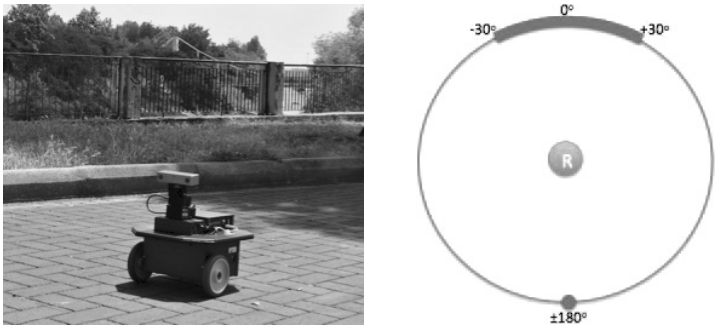

(a) (b)

Fig. 1. (a) Stereo camera-equipped mobile robotic platform and (b) floor plan of the robot's environment.

The outcome of this work is a computationally effective, solely based on vision, and, at the same time, reliable fuzzy obstacle avoidance method for use in autonomously moving robots. Furthermore, the proposed method is independent of the robotic platform used. No complex sensory arrangement is required. The sole presence of a stereo camera sensor, which is available in most of the humanoid robots, serves the purposes of this work effectively, as it happens in nature with humans.

2. Stereo Vision

Contrary to most of the stereo algorithms, which directly use the camera's images,[15] the proposed stereo algorithm uses an enhanced version of the captured images as input. The initially captured images are processed in order to extract the edges in the depicted scene. The utilized edge detecting method is the Laplacian of Gaussian (LoG), using a zero threshold. This choice produces the maximum possible edges. The LoG edge detection method smoothens the initial images with a Gaussian filter in order to suppress any possible noise. Then, a Laplacian kernel is applied that marks regions of significant intensity change. Actually, the combined LoG filter, with standard deviation equal to 2, is applied at once and the zero crossings are found. The extracted edges are, afterwards, superimposed to the initial images. The steps of the aforementioned process are shown in Fig. 2. The outcome of this procedure is a new version of the original images having more striking features and textured surfaces, which facilitate the following stereo matching procedure.

The depth maps are computed using a three-stage local stereo correspondence algorithm. The utilized stereo algorithm combines low computational complexity with sophisticated data processing. Consequently, it is able to produce dense disparity maps of good quality in frame rates suitable for robotic applications. The main attribute that differentiates this algorithm from the majority of the other ones is that the matching cost aggregation step consists of a sophisticated

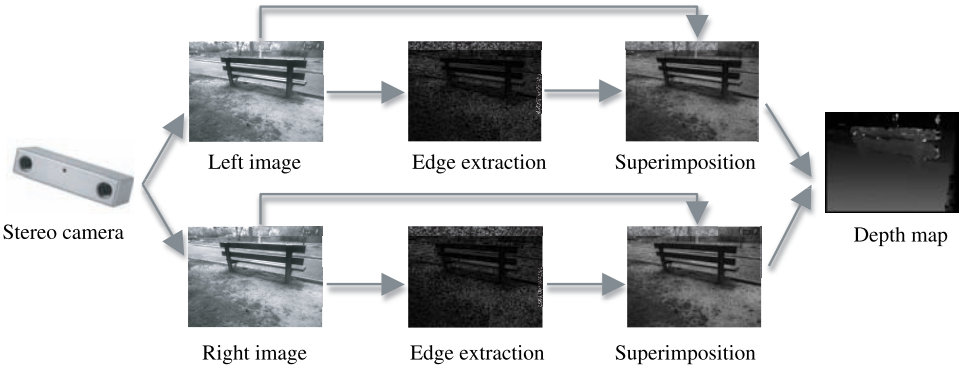

Fig. 2. Image enhancement steps of the proposed stereo algorithm.

Gaussian-weighted rather than a simple summation. Furthermore, the disparity selection step is a winner-takes-all (WTA) choice, as the absence of any iteratively updated selection process significantly reduces the computational payload of the overall algorithm. Finally, any dedicated refinement step is also absent for speed reasons.

The matching cost function utilized is the truncated absolute differences (AD). AD is inherently the simplest metric of all, involving only summations and finding absolute values. The AD are truncated if they excess the 4% of the maximum intensity value. Truncation suppresses the influence of noise in the final result. This is very important for stereo algorithms that are intended to be applied to outdoor scenes. Outdoor pairs usually suffer from noise induced by a variety of reasons, e.g. lighting differences and reflections. For every pixel of the reference (left) image, AD are calculated for each of its candidate matches in the other (right) image.

$$AD(x, y, d) = |I_{\text{left}}(x, y) - I_{\text{right}}((x - d), y)|\,, \tag{1}$$

where I_{left} and I_{right} denote the intensity values for the left and right image respectively, d is the value of the disparity under examination ranging for 0 to $D-1$, and x, y are the coordinates of the pixel on the i, j plane.

The computed matching costs for every pixel and for all its potential disparity values comprise a 3D matrix, usually called as disparity space image (DSI). The DSI values for constant disparity value are aggregated inside fix-sized square windows. The dimensions of the chosen aggregation window play an important role in the quality of the final result. Generally, small dimensions preserve details but suffer from noise. On the contrast, large dimensions may not preserve fine details but significantly suppress the noise. This behavior is highly appreciated in outdoor robotic applications where noise is a major factor, as already discussed. The aggregation windows dimensions used in the proposed algorithm are 19×19 pixels. This choice is a compromise between real-time execution speed and noise cancelation. The AD aggregation step of the proposed algorithm is a weighted summation. Each pixel is assigned a weight depending on its Euclidean distance from the central pixel. A 2D Gaussian function determines the weights value for each pixel. The center of the function coincides with the central pixel. The standard deviation is equal to the one-third of the distance from the central pixel to the nearest window-border. The applied weighting function can be calculated once and then be applied to all the aggregation windows without any further change. Thus, the computational load of this procedure is kept within reasonable limits.

$$DSI(x, y, d) = \sum_{i=-w}^{w} \sum_{j=-w}^{w} gauss(i, j) \cdot AD(x, y, d), \tag{2}$$

where, the pixel ranges $[-w, w]$ define the weighted aggregation window.

Finally, the optimum disparity value for each pixel, i.e. the disparity map, is chosen by a simple and noniterative WTA step. In the resulting disparity maps,

smaller values indicate more distant objects, while bigger disparity values indicate objects lying closer.

$$disp(x, y) = arg(\min(DSI(x, y, d))). \tag{3}$$

As a result, the disparity maps are equivalent to depth maps of the depicted scene and can be used directly for the subsequent obstacle analysis.

3. Fuzzy Obstacle Analysis and Direction Decision

The previously calculated depth maps are used to extract useful information about the navigation of the robot. In contrast to many implementations that involve complex calculations upon the disparity maps, the proposed decision-making algorithm is focused on computational efficiency. This is feasible due to the absence of significant noise in the produced disparity maps. The goal of the obstacle analysis module is to assess the traversablity of three possible directions of movement, i.e. forward, left, and right. In order to achieve that the developed method divides each disparity map into three equally sized windows, as in Fig. 3.

The division of the disparity map excludes the boundary regions, in this case a peripheral frame of 20 pixels width, because the disparity calculation in such regions is often problematic. In each window, the pixels p whose disparity value $D(p)$ is greater than a defined threshold value *Thres* are enumerated. The enumeration results are normalized toward the widow's pixels population and then examined. The more traversable the corresponding direction is the smaller the enumeration result should be. Thus, the traversability of the left, central, and right window, respectively T_L, T_C, and T_R, is assessed.

The values of the parameter *Thres* play an important role to the algorithm's behavior. Small values of *Thres* favor hesitancy in moving forward, ensuring obstacle

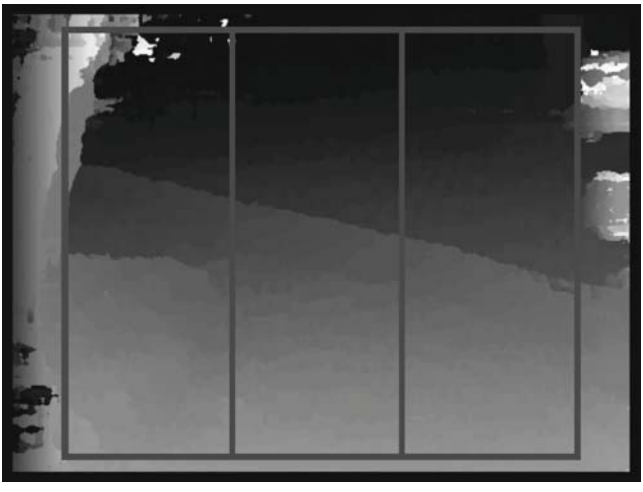

Fig. 3. Depth map's division in three windows.

avoidance but at the same time being susceptible to false alarms due to noise. On the other hand, the opposite scenario is less susceptible to false alarms but may be proven risky for the robot. In this work, the value $Thres = 120$ was chosen after exhaustive experimentation as a fair compromise between the two extreme behaviors.

The results of the traversability estimation for the three windows, i.e. the left, central, and right one, are used as the three input values of an FIS that decides the proper direction of movement for the robot. The outputs of the FIS are the angle of the direction that the robot should follow and an indicator that the robot should move backwards. Figure 4 shows the membership functions (MF) for the three inputs (all having identical MF, which is shown in Fig. 4(a)) and the two outputs (Figs. 4(b) and 4(c)).

A direction angle of 0° indicates forward movement, negative angles indicate movement toward left, and positive angles indicate movement toward right. The second output variable indicates that the robot should move backwards in order to acquire a broader view of the scene. This should happen if all the possible directions within the robot's field of view are, or at least seem, nontraversable.

The set of fuzzy rules that were used for the FIS is:

- IF ("T_L" is "Large" AND "T_C" is not "Large" AND "T_R" is not "Large") THEN "Angle" is "Left."

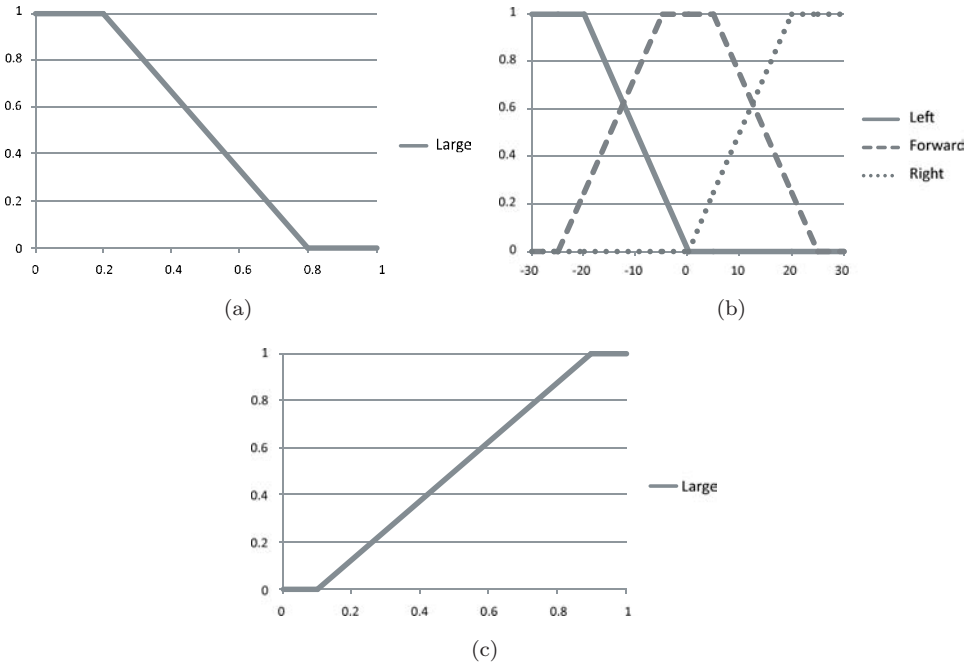

Fig. 4. Fuzzy membership functions: (a) input MF: traversability of the left/central/right window, (b) output MF: direction angle, and (c) output MF: "move backwards" indicator.

- IF ("T_L" is not "Large" AND "T_C" is "Large" AND "T_R" is not "Large") THEN "Angle" is "Forward."
- IF ("T_L" is not "Large" AND "T_C" is not "Large" AND "T_R" is "Large") THEN "Angle" is "Right."
- IF ("T_L" is not "Large" AND "T_C" is not "Large" AND "T_R" is not "Large") THEN "move backwards" is "Large."

This small set of simple rules is enough to ensure that the robot will adapt its direction of movement so as to avoid any obstacles in its way. Experimental validation of the proposed system indicated that the option to move back should actually be adopted when the "move backwards" output of the FIS is larger than 0.65 (see Fig. 4(c)). Of course, this value was determined empirically and smaller or bigger values could be used instead, resulting in more "brave" or hesitant behaviors respectively.

4. Experimental Results

The presented method was tested on image pairs acquired by the robot shown in Fig. 1(a). The image pairs were captured in real-life outdoor environments under natural lighting conditions. The experimental results presented in this section cover various situations of different complexity that the robot had to deal with. For each case, the two stereo input images and the computed disparity map are given. Subsequently, the values of the FIS's input and output variables are also given in respective tables.

Figure 5 shows cases where the robot has decided to move exactly forward. This decision was taken even in the cases of Figs. 5(a), 5(e)–5(g), 5(i), and 5(l). Such cases where there is an obvious obstacle in the robot's way may lead vision-based obstacle avoidance algorithms to nonoptimal decisions. The minimum distance beyond which the obstacle should be avoided is controlled in the proposed method by the parameter *Thres*, as mentioned in Sec. 3. It is evident that the robot effectively treats the obstacles as not harmful up to a certain point, before it decides to steer away from them. Table 1 gives the values of the FIS's input and output variables for the image pairs of Fig. 5, where the robot decided to move exactly forward.

The disparity maps obtained by stereo vision, almost inevitably, contain erroneously estimated regions, as also inferred by the popular online stereo algorithms' test bench.[30] Such inaccuracies are also present in the disparity maps produced by the proposed method. The majority of the obstacle avoidance algorithms, including the ones covered in the introduction,[18,19,21,22] are based on highly accurate and noise-free depth estimations. As a consequence, a solely vision-based obstacle avoidance method could not have used any of the aforementioned algorithms. On the contrary, the proposed algorithm can tolerate such problems as shown by the experimental results.

Figure 6 shows instances where the robot decided to steer left by some angle. Table 2 gives the values of the FIS's input and output variables for the image

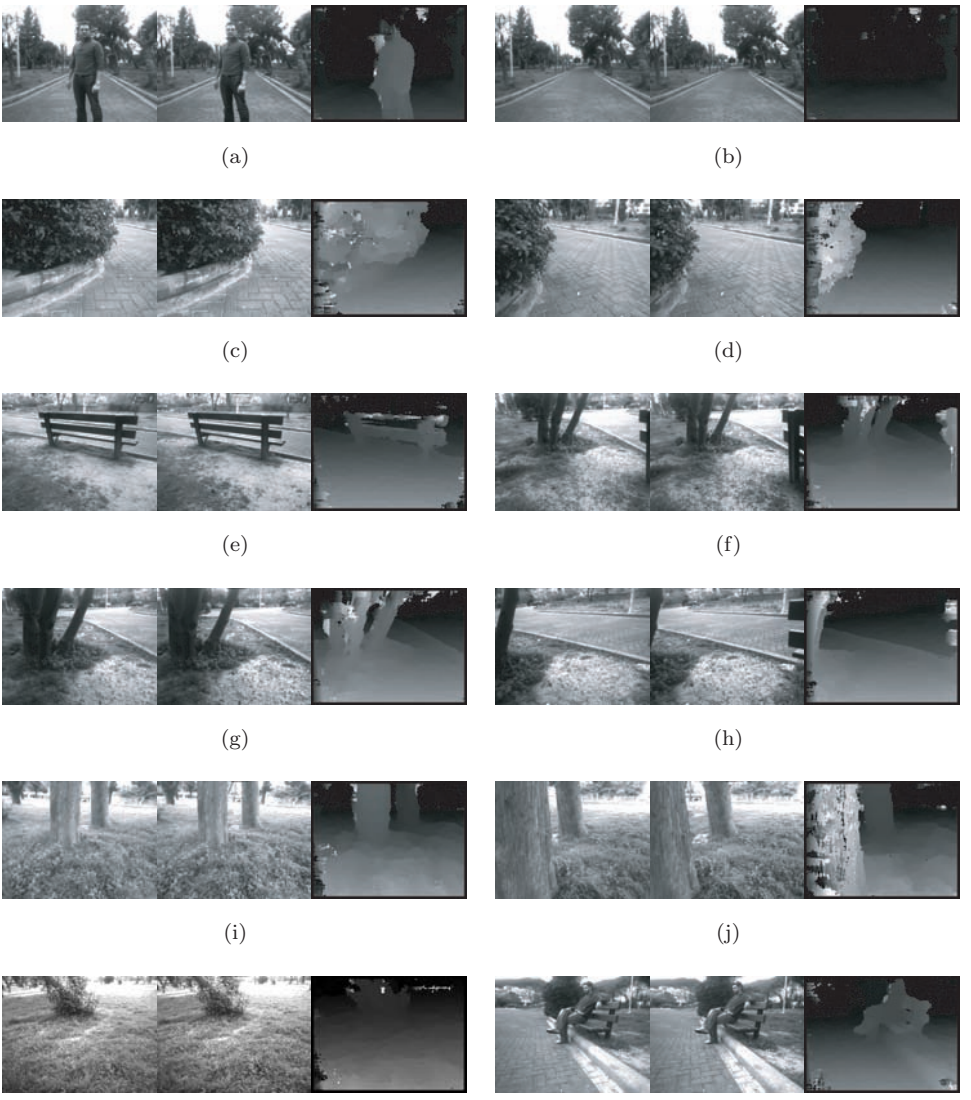

Fig. 5. Test images and disparity maps where the algorithm chose to move forward.

pairs of Fig. 6, where the robot decided to steer left, as indicated by the angles' negative sign. The exact steering angle varies according to the scene's details instead of being constant, as it happens with other methods. The presented algorithm is able to cope with scenes resulting in significantly problematic disparity maps, as in Fig. 6(c). Even in this case, where the computed disparity map contains several extended erroneously computed regions, the fuzzy direction decision algorithm takes the correct decision.

Table 1. Results for the cases where the algorithm chose to move forward.

Image Pair Figures	Inputs			Outputs	
	Left (%)	Central (%)	Right (%)	Angle (deg)	"Move Backwards"
5(a)	0.03	1.68	1.14	0.0	0.50
5(b)	0.03	0.02	0.80	0.0	0.50
5(c)	19.82	9.82	5.87	0.0	0.50
5(d)	54.05	5.65	5.23	0.0	0.50
5(e)	4.95	6.00	3.91	0.0	0.50
5(f)	5.20	8.16	9.34	0.0	0.50
5(g)	20.71	15.21	10.52	0.0	0.50
5(h)	18.72	11.65	15.38	0.0	0.50
5(i)	13.06	14.60	9.01	0.0	0.50
5(j)	71.42	16.05	4.83	0.0	0.50
5(k)	9.84	8.44	8.08	0.0	0.50
5(l)	0.85	0.13	3.81	0.0	0.50

(a) (b)

(c) (d)

Fig. 6. Test images and disparity maps where the algorithm chose to move left.

Table 2. Results for the cases where the algorithm chose to move left.

Image Pair Figures	Inputs			Outputs	
	Left (%)	Central (%)	Right (%)	Angle (deg)	"Move Backwards"
6(a)	8.75	89.62	44.53	−17.1	0.50
6(b)	9.71	37.54	43.81	−16.6	0.50
6(c)	22.86	38.60	43.37	−12.0	0.56
6(d)	3.94	73.83	82.03	−19.0	0.50

Figure 7 shows cases where the robot decided to steer right by some angle and Table 3 gives the values of the FIS's input and output variables for the corresponding image pairs. As shown by the value of the parameter "move backwards" for the pairs of Figs. 6(c) and 7(d), there is a relatively high tendency to adopt the option to move backwards in these cases. However, since the threshold value had been set to 0.65, the robot chose to steer left and right respectively. On the other hand, Fig. 8

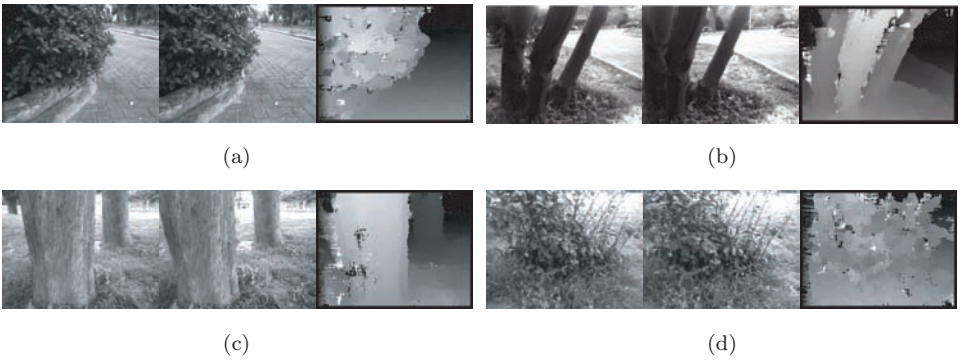

(a) (b)

(c) (d)

Fig. 7. Test images and disparity maps where the algorithm chose to move right.

Table 3. Results for the cases where the algorithm chose to move right.

Image Pair Figures	Inputs			Outputs	
	Left (%)	Central (%)	Right (%)	Angle (deg)	"Move Backwards"
7(a)	81.45	66.78	7.62	+18.6	0.50
7(b)	83.79	85.95	14.94	+19.3	0.50
7(c)	67.27	80.19	9.28	+18.6	0.50
7(d)	67.83	67.51	36.54	+9.1	0.61

Fig. 8. Test images and disparity map where the algorithm chose to move backwards.

and Table 4 show a scene and the respective FIS variables where the robot actually decided to move backwards. Other threshold value for the "move backwards" parameter would had lead to other behaviors for the last three cases. The inherent ability of the algorithm to decide whether the robot should move backwards prevents entrapments into local minima, which often happens in methods such as the virtual force field[19] and the elastic strips.[21]

As shown by the experimental results, the proposed algorithm has succeeded in deciding an obstacle avoiding direction of movement for a variety of scenes. It

Table 4. Results for the cases where the algorithm chose to move backwards.

Image Pair Figure	Inputs			Outputs	
	Left (%)	Central (%)	Right (%)	Angle (deg)	"Move Backwards"
8	70.94	87.21	73.51	−2.6	0.69

manages to process even erroneous vision data without the need of further sensors' input. The used FIS decides the exact value of the steering angle in an continuous manner. In this sense, the proposed method combines attributes of the methods presented in Refs. 4 and 25 while adding further capabilities and maintaing the computational load in very low levels.

5. Conclusion

For mobile robots to move toward human-like behaviors, autonomous navigation is an essential milestone. Obstacle avoidance, using a minimum of sensory and processing resources, is the first step to this direction.

This work has presented an obstacle avoidance method for stereovision-equipped mobile robots. The proposed method is based on a custom developed stereo algorithm and a simple but effective fuzzy obstacle analysis and direction decision module. Both these modules are focused on avoiding complex calculation methodologies. In accordance with its biological archetypes, the robot executing the proposed algorithm has effectively detected and avoided any obstacles using only stereovision as input.

The behavior of the method has been validated by real outdoor data sets of various scenes. The algorithm exhibits robust behavior and is able to ensure collision-free autonomous mobility to robots. Moreover, the robot's direction changes are smooth, resembling that of living creatures, due to the fuzzy system's continuous range of output values.

References

1. R. A. Russell, G. Taylor, L. Kleeman and A. H. Purnamadjaja, Multi-sensory synergies in humanoid robotics, *International Journal of Humanoid Robotics* **1**(2) (2004) 289–314.
2. F. Santini, R. Nambisan and M. Rucci, Active 3D vision through gaze relocation in a humanoid robot, *International Journal of Humanoid Robotics* **6**(3) (2009) 481–503.
3. J. S. Gutmann, M. Fukuchi and M. Fujita, A floor and obstacle height map for 3D navigation of a humanoid robot, in *IEEE International Conference on Robotics and Automation* (2005), pp. 1066–1071.
4. K. Sabe, M. Fukuchi, J. S. Gutmann, T. Ohashi, K. Kawamoto and T. Yoshigahara, Obstacle avoidance and path planning for humanoid robots using stereo vision, in *IEEE International Conference on Robotics and Automation* (2004), Vol. 1, pp. 592–597.
5. L. Iocchi and K. Konolige, A multiresolution stereo vision system for mobile robots, in *Italian AI Association Workshop on New Trends in Robotics Research* (1998).
6. R. Siegwart and I. R. Nourbakhsh, *Introduction to Autonomous Mobile Robots* (MIT Press, Massachusetts, 2004).
7. O. Schreer, Stereo vision-based navigation in unknown indoor environment, in *5th European Conference on Computer Vision* (1998), Vol. 1, pp. 203–217.
8. D. Scharstein and R. Szeliski, A taxonomy and evaluation of dense two-frame stereo correspondence algorithms, *International Journal of Computer Vision* **47**(1–3) (2002) 7–42.

9. P. H. S. Torra and A. Criminisi, Dense stereo using pivoted dynamic programming, *Image and Vision Computing* **22**(10) (2004) 795–806.
10. K. Muhlmann, D. Maier, J. Hesser and R. Manner, Calculating dense disparity maps from color stereo images, an efficient implementation, *International Journal of Computer Vision* **47**(1–3) (2002) 79–88.
11. L. Di Stefano, M. Marchionni and S. Mattoccia, A fast area-based stereo matching algorithm, *Image and Vision Computing* **22**(12) (2004) 983–1005.
12. S. Yoon, S. K. Park, S. Kang and Y. K. Kwak, Fast correlation-based stereo matching with the reduction of systematic errors, *Pattern Recognition Letters* **26**(14) (2005) 2221–2231.
13. C. Zach, K. Karner and H. Bischof, Hierarchical disparity estimation with programmable 3D hardware, in *International Conference in Central Europe on Computer Graphics, Visualization and Computer Vision* (2004), pp. 275–282.
14. K. J. Yoon and I. S. Kweon, Adaptive support-weight approach for correspondence search, *IEEE Transactions on Pattern Analysis and Machine Intelligence* **28**(4) (2006) 650–656.
15. L. Nalpantidis, G. C. Sirakoulis and A. Gasteratos, Review of stereo vision algorithms: From software to hardware, *International Journal of Optomechatronics* **2**(4) (2008) 435–462.
16. J. Borenstein and Y. Koren, Real-time obstacle avoidance for fast mobile robots in cluttered environments, *IEEE Transactions on Systems, Man, and Cybernetics* **19**(5) (1990) 1179–1187.
17. A. Ohya, A. Kosaka and A. Kak, Vision-based navigation of mobile robot with obstacle avoidance by single camera vision and ultrasonic sensing, *IEEE Transactions on Robotics and Automation* **14**(6) (1998) 969–978.
18. P. Moravec, Certainty grids for mobile robots, in *NASA/JPL Space Telerobotics Workshop* (1987), Vol. 3, pp. 307–312.
19. J. Borenstein and Y. Koren, The vector field histogram-fast obstacle avoidance for mobile robot, *IEEE Transactions on Robotics and Automation* **7**(3) (1991) 278–288.
20. O. Khatib, Motion coordination and reactive control of autonomous multi-manipulator system, *Journal of Robotic Systems* **15**(4) (1996) 300–319.
21. O. Khatib, Robot in human environments: Basic autonomous capabilities, *International Journal of Robotics Research* **18**(7) (1999) 684–696.
22. C. Kyung Hyun, N. Minh Ngoc and R. M. Asif Ali, A real time collision avoidance algorithm for mobile robot based on elastic force, *International Journal of Mechanical, Industrial and Aerospace Engineering* **2**(4) (2008) 230–233.
23. A. Manz, R. Liscano and D. Green, A comparison of realtime obstacle avoidance methods for mobile robots, in *Experimental Robotics II* (Springer-Verlag, 1993), pp. 299–316.
24. V. Kunchev, L. Jain, V. Ivancevic and A. Finn, Path planning and obstacle avoidance for autonomous mobile robots: A review, in *International Conference on Knowledge-Based and Intelligent Information and Engineering Systems* (Springer-Verlag, 2006), Vol. 4252 of LNCS, pp. 537–544.
25. P. Reignier, Fuzzy logic techniques for mobile robot obstacle avoidance, *Robotics and Autonomous Systems* **12**(3–4) (1994) 143–153.
26. J. Vandorpe, H. Van Brussel and H. Xu, Exact dynamic map building for a mobile robot using geometrical primitives produced by a 2D range finder, in *IEEE International Conference on Robotics and Automation* (Minneapolis, USA, 1996), pp. 901–908.

27. R. Labayrade, D. Aubert and J. P. Tarel, Real time obstacle detection in stereovision on nonflat road geometry through "V-disparity" representation, in *IEEE Intelligent Vehicle Symposium* (Versailles, France, 2002), Vol. 2, pp. 646–651.
28. J. Zhao, J. Katupitiya and J. Ward, Global correlation based ground plane estimation using V-disparity image, in *IEEE International Conference on Robotics and Automation* (Rome, Italy, 2007), pp. 529–534.
29. N. Soquet, D. Aubert and N. Hautiere, Road segmentation supervised by an extended V-disparity algorithm for autonomous navigation, in *IEEE Intelligent Vehicles Symposium* (Istanbul, Turkey, 2007), pp. 160–165.
30. D. Scharstein and R. Szeliski, http://vision.middlebury.edu/stereo/ (2010).

Lazaros Nalpantidis was born in Thessaloniki, Greece, in 1980. He received the B.Sc. degree in Physics and the M.Sc. degree (with honors) in electronic engineering from the Aristotle University of Thessaloniki, in 2003 and 2005, respectively. He is currently with the Laboratory of Robotics and Automation, Department of Production and Management Engineering, Democritus University of Thrace, where he is currently pursuing the Ph.D. degree in the field of robotic vision.

Lazaros Nalpantidis has been and is currently participating in various European and national research projects. He has served as a reviewer for various international journals and conferences and is coauthor of 19 scientific papers in various conferences and workshops, and six in international journals. His current research interests include vision systems for robotic applications and signal/image processing systems' design.

Antonios Gasteratos is an assistant professor at the Department of Production and Management, Democritus University of Thrace, Greece. He teaches the courses of "robotics," "automatic control systems," "measurements technology," and "electronics." He holds a B.Eng. and a Ph.D. from the Department of Electrical and Computer Engineering, DUTH, Greece. During 1999–2000, he was a visiting researcher at the Laboratory of Integrated Advanced Robotics (LIRA-Lab), DIST, University of Genoa, Italy, with a TMR grant from VIRGO and SMART networks.

Antonios Gasteratos has served as a reviewer to numerous of scientific journals and international conferences. His research interests are mainly in mechatronics and in robot vision. He has published more than 60 papers in books, journals, and conferences. He is a member of the IEEE, IAPR, ECAI, and the Technical Chamber of Greece (TEE). He is a member of EURON, euCognition, and I*Proms networks. More details about him are available at http://robotics.pme.duth.gr/.